HHS Public Access

Author manuscript

Clin Cancer Res. Author manuscript; available in PMC 2020 August 01.

Published in final edited form as:

Clin Cancer Res. 2020 February 01; 26(3): 690–703. doi:10.1158/1078-0432.CCR-19-1486.

Colony-stimulating Factor 1 Receptor (CSF1R) Activates AKT/mTOR Signaling and Promotes T-cell Lymphoma Viability

Carlos Murga-Zamalloa[1,2], **Delphine Rolland**[3], **Avery Polk**[1], **Ashley Wolf**[1], **Hiran M. Dewar**[1], **Pinki Chowdhury**[1], **Ozlem Onder**[3], **Rajan Dewar**[2], **Noah Brown**[2], **Nathanael G. Bailey**[4], **Kedar Inamdar**[5], **Megan S. Lim**[3], **Kojo S.J. Elenitoba-Johnson**[3], **Ryan A. Wilcox**[2]

[(1)]Department of Internal Medicine, University of Michigan, Ann Arbor, Michigan.

[(2)]Pathology, University of Michigan, Ann Arbor, Michigan.

[(3)]Department of Laboratory Sciences, University of Pennsylvania, Philadelphia, Pennsylvania.

[(4)]Department of Pathology, University of Pittsburgh, Pittsburgh, Pennsylvania.

[(5)]Department of Pathology, Henry Ford Hospital, Detroit, Michigan.

Abstract

Purpose: Peripheral T-cell lymphomas are clinically aggressive and usually fatal, as few complete or durable remissions are achieved with currently available therapies. Recent evidence supports a critical role for lymphoma-associated macrophages during T-cell lymphoma progression, but the specific signals involved in the cross-talk between malignant T-cells and their microenvironment are poorly understood. Colony-stimulator factor 1 receptor (CSF1R, CD115) is required for the homeostatic survival of tissue-resident macrophages. Interestingly, it's aberrant expression has been reported in a subset of tumors. In this manuscript we evaluated its expression and oncogenic role in T-cell lymphomas.

Experimental Design: Loss-of-function studies, including pharmacologic inhibition with a clinically available tyrosine-kinase inhibitor, pexidartinib, were performed in multiple in vitro and in vivo models. In addition, proteomic and genomic screenings were performed to discover signaling pathways that are activated downstream of CSF1R signaling.

Results: We observed that CSF1R is aberrantly expressed in many T-cell lymphomas, including a significant number of peripheral and cutaneous T-cell lymphomas. Colony-stimulating factor 1 (CSF1), in an autocrine or paracrine-dependent manner, leads to CSF1R autophosphorylation and activation in malignant T-cells. Furthermore, CSF1R signaling was associated with significant changes in gene expression and in the phosphoproteome, implicating PI3K/AKT/mTOR in

Corresponding authors: Ryan A. Wilcox, MD, PhD, University of Michigan, 1500 East Medical Center Drive, 4310 Rogel Cancer Center, Ann Arbor, MI 48109., Phone: 734-647-8901, Fax: 734-647-8664, rywilcox@med.umich.edu, Carlos A. Murga-Zamalloa, MD, University of Michigan, 1500 East Medical Center Drive, 4310 Rogel Cancer Center, Ann Arbor, MI 48109., Phone: 734-763-3960, carlosmu@med.umich.edu.

Authors contributions

R.W. and C.M.Z. designed and conducted research experiments, acquired and analyzed data, and wrote the manuscript. D.R. conducted, designed and analyzed research experiments. P.C., H.D., A.W., A.P., N.B., K.I. R.D. O.O., conducted experiments. M.L. and K.E.J. provided reagents and analyzed data.

Conflict of interest: The authors have declared that no conflict of interest exists.

CSF1R-mediated T-cell lymphoma growth. We also demonstrated that inhibition of CSF1R in-vivo and in-vitro models is associated with decreased T-cell lymphoma growth.

Conclusions: Collectively, these findings implicate CSF1R in T-cell lymphomagenesis and have significant therapeutic implications.

Keywords

CSF1R; tumor microenvironment; T-cell lymphomas; tumor associated macrophages; mTOR; pexidartinib; PI3K inhibitor; tenalisib

INTRODUCTION

Peripheral T-cell lymphomas (PTCL) are a heterogeneous group of non-Hodgkin lymphomas that are characterized by an aggressive clinical course, chemotherapy resistance, and poor survival(1–5). While cell surface receptors, including cytokine receptors and the T-cell receptor(6), play critical roles during T-cell lymphoma (TCL) progression and may be therapeutically targeted, the paucity of representative cell lines and animal models has hampered progress, and PTCL remains an area of unmet need. The sequential steps involved in the maturation and activation of normal T-cells are tightly regulated by cues derived from their microenvironment. Not surprisingly, communication between malignant T-cells and constituents of their microenvironment, including macrophages, is critical for tumor growth, survival and migration(3,7–11). Lymphoma-associated macrophages (LAM) are abundant constituents of the TCL microenvironment, and have emerged as an attractive therapeutic target(3,12,13).

Colony-stimulating factor 1 receptor (CSF1R) is required for the homeostatic survival and migration of macrophages and their progenitors(14–16). In addition to its expression on myeloid-lineage cells, including macrophages(17), Langerhan's cells(18), osteoclasts(19), and tumor-associated macrophages(20), CSF1R expression has also been observed on non-hematopoietic cells, including Paneth cells(21) and many solid tumors (20,22–25). CSF1R activation occurs upon binding one of its two ligands: colony-stimulating factor 1 (CSF1) and interleukin-34 (IL-34)(26). Although both ligands are partially redundant, CSF1 is a dominant trophic factor for macrophages(27–30), including tumor-associated macrophages(31). CSF1R belongs to the platelet-derived growth factor receptor (PDGFR) family, and is a type III receptor tyrosine kinase(32). Upon ligand engagement, CSF1 receptors dimerize, leading to step-wise auto-phosphorylation of tyrosine residues within the cytoplasmic tail and recruitment of signaling proteins, including PI3K(33,34). More recently it has been demonstrated that paracrine activation on CSF1R-expressing carcinoma cells activates oncogenic pathways that promote tumor invasion(31,35). Also, autocrine activation of CSF1R in breast carcinoma is associated with tumor metastasis and growth(36), and poor outcomes(20,37).

The aberrant expression of CSF1R has also been demonstrated in lymphoid neoplasms, particularly classic Hodgkin lymphoma(12,38–41). CSF1R expression in Hodgkin lymphoma results from dysregulated epigenetic control and loss of methylation within an alternative CSF1R promoter, resulting in the expression of 'non-canonical' CSF1R

transcripts(39). Importantly, CSF1R inhibition with selective tyrosine kinase inhibitors is a rational therapeutic approach in neoplasms that aberrantly express CSF1R(22,25,42). Given the pathogenic role of CSF1R-expressing LAM in the TCL and the availability of CSF1R antagonists, we evaluated the expression and function of CSF1R in the T-cell lymphomas. We adopted an unbiased phosphoproteomic approach, demonstrating that CSF1R activation in T-cell lymphomas leads to AKT/mTOR activation and promotes tumor growth. Therefore, CSF1R inhibition is a rational therapeutic strategy in the TCL, with a dual mechanism of action in CSF1R+ TCL.

Material and Methods

Immunohistochemistry

Immunohistochemical stains were performed on selected cases using tissue microarrays or whole tissue sections. CSF1R immunohistochemical stains were performed with two antibodies; rabbit anti-CSF1R (Santa Cruz Biotechnologies H-300, dilution 1:100) and rabbit anti-CSF1R (Abcam EPR20634, dilution 1:200). Immunohistochemical staining was performed at two independent laboratories (Michigan State University Histolab, and University of Michigan Cancer Center histology core). CSF1R expression was validated in classical Hodgkin and non-Hodgkin lymphomas (supplementary figure 1A and data not shown), both antibodies showed similar results. Cases were graded as positive for CSF1R if more than 30% of tumor cells expressed cytoplasmic CSF1R. Interpretation of CSF1R expression was performed independently by three pathologists (C.M.Z, K.I. and N.G.B). CBFA2T3 immunohistochemical stains were performed with rabbit anti-CBFA2T3 (PA5–66808, dilution 1:1000 – Thermo Scientific), as described(43). For nuclear expression of CBFA2T3, the percentage of positive tumor cells, and the intensity (0–3) were measured. The h-score was calculated (0–300), and loss of CBFA2T3 was scored if the h-score was less than 150 (less than 0.5 standard deviations from the mean). Tumor samples analyzed were collected from the pathology library of cases at the University of Michigan Health System. Cutaneous T-cell lymphoma (CTCL) cases represent primary cutaneous CD30-positive lymphoproliferative disorders (n=31) and mycosis fungoides (n=23).

Cell culture and shRNA lentiviral transduction

ALCL-cell derived cell lines (SR786, Karpas290, SUP-M2, SUDH1L and DEL), CTCL-derived cell lines (MyLa, Mac-1), and PTCL-NOS (T8ML1) derived cell lines were maintained in RPMI-1640 with 10% fetal bovine serum. Cell lines were validated, as previously described(18,43,44), and tested for mycoplasma every 6 months by Universal Mycoplasma Detection Kit (ATCC). T8ML1 cell lines were generated from a PTCL, NOS patient(45), and maintained with supplemented IL-2 RPM1 media. Stable expression of doxycycline-inducible shRNA was generated with lentiviral mediated transduction of plko-Tet-On vectors. Oligo sequences for CSF1R shRNA#1: CCGGACAGGAGAGAGCGGGACTATACTCGAGTATAGTCCCGCTCTCTCCTGTTTTTTG, shRNA#2: CCGGGAATCTCACAGGACCTCTTAGCTCGAGCTAAGAGGTCCTGTGAGATTCTTTTTTG and scramble: CCGGCCTAAGGTTAAGTCGCCCTCGCTCGAGCGAGGGCGACTTAACCTTAGGTTT

TT. Knock-down of CBFA2T3 was performed with sigma mission pLKO.1 shRNA vectors, TRCN0000020164 (shRNA #1) and TRCN0000020165 (shRNA #2).

Compounds

Crizotinib was purchased from Selleckchem. PLX3397/Pexidartinib was provided under MTA from Plexxikon Inc. Tenalisib/RP6530 was provided under MTA from Rhizen pharmaceuticals. Unless otherwise indicated in the manuscript, inhibitory compounds were used at 1μM final concentration and vehicle control (DMSO) used as an appropriate control. Human recombinant purified CSF1 was acquired from BioLegend. Induction of CSF1R signaling with recombinant CSF1 ligand was done at 20ng/ml concentration at indicated times.

Antibodies, ELISA assay and quantitative real-time PCR

Complete list of antibodies is included supplemental table 5. ELISA assays for CSF1R and pan-phosphorylated CSF1R were purchased from RayBiotech and performed according to manufacturer instructions. ELISA assays for quantification of CSF1 ligand were purchased from RayBiotech, and performed according to manufacturer's instructions. List of primers for quantitative real-time PCR primers are included in supplemental table 6.

Proliferation, apoptosis and colony formation assays

Colony formation assays were performed with Methocult H4230 (Stem cell technologies) per manufacturer's instructions. Briefly, approximately 5000 cells were seeded with or without doxycycline (10ng/ml), colonies were grown for 7 days before staining with p-iodonitrotetrazolium chloride (Sigma-Aldrich, St. Louis, MO). Proliferation was evaluated with CellTiter Glo assays (Promega) over 72 hours. Multiparametric evaluation of cellular apoptosis was performed by flow cytometry analysis of Annexin V (Invitrogen) incorporation, coupled with either Propidium Iodide (Miltenyi Biotec – MACS) or DilC1(5) incorporation (Thermo Scientific). Staining and detection procedures for flow cytometry were performed according to manufacturer instructions.

Phosphoproteome analysis by mass spectrometry

Sixty million cells were lysed in 9 M urea/20 mM HEPES pH8.0/0.1% SDS and a cocktail of phosphatase inhibitors. Six milligrams of protein were reduced with 4.5 mM DTT, alkylated with 10 mM iodoacetamide and then digested with trypsin (1/50, w/w) overnight at 37°C. Metal oxide affinity chromatography (MOAC) was performed to enrich phosphorylated peptides and reduce the sample complexity prior to tyrosine-phosphorylated peptide immunoprecipitation as previously described (46). Peptides were analyzed in an Orbitrap FusionTM TribidTM mass spectrometer (Thermo Fisher). RAW files were processed in MaxQuant version 1.6.0.1 using default setting if not stated otherwise (47). Peptides and proteins were identified with a target-decoy approach in revert mode using Andromeda search engine integrated into the MaxQuant environment. The search was performed against the human UniProt FASTA databased (April 2016). Oxidized methionine, protein N-acetylation and serine/threonine/tyrosine phosphorylation were selected as variable modifications and carbamidomethyl cysteine was selected as fixed modification.

Enzyme specificity was set to trypsin and up to two missed cleavages were allowed for protease digestion. The false-discovery rate (FDR) at the protein, peptide and modification levels was set to 1%. The “match between runs” option was enabled.

Gene expression profiling

Microarray based gene expression profiling was performed on Karpas 299 after 6hrs treatment with DMSO, pexidartinib or crizotinib at the University of Michigan DNA sequencing core. Analysis of the data, was performed with the oligo package of bioconductor, in order to fit $\log_2$ transformed expression values to the probesets. Limma was used in order to fit weighted linear models to the data and look for genes of interest. Detailed protocol and statistics are included as supplemental methods.

Mouse studies

Mouse studies were approved by the University Committee on Care and Use of Animals (UCUCA) and performed in accordance with guidelines established by the Unit for Laboratory Animal Medicine (ULAM) at the University of Michigan. Mice were housed under specific-pathogen free conditions. SUPM2 or Karpas 299 cells (2×10^6) were injected subcutaneously in immunodeficient NSG mice or Rag2/Il2rg immunodeficient mice with transgenic expression of humanized CSF1 ligand(48). Upon injections, mice were fed with either nutritionally complete pexidartinib-containing (275mg PLX3397/kg) or control chow, provided under MTA by Plexxikon. Toxicity secondary to drug delivery was assessed by daily monitoring of clinical condition (appearance, activity and body condition). Tumors were measured and mice humanely euthanized approximately 14 days after pexidartinib- or control-treatment.

Statistics

All the data represents at least three independent experiments. Sample size for animal experiments was based on previous publications performing similar experiments, ensuring that a sufficient sample size was selected to confidently assess statistical significance(6). Treatment allocation was not randomized, and all animals in a given experiment were included for analysis. Significance was calculated with parametric student T-test. Statistics for gene expression profiling analysis are indicated in supplemental methods section. Phosphoproteomic bioinformatic analysis was conducted in Perseus (version 1.6.2.3) and Microsoft Excel. The dataset was transformed into a log2 scale. To overcome the “missing value” issue, a stringent valid value filtering was performed. These required at least 30% of valid values in all groups and at least 2/3 of valid values in at least one group. The remaining missing values were included from a random Gaussian-shaped distribution applying a downshift of 1.5 times the standard deviation of the global dataset, and a width of 0.5 times the standard deviation. The data was normalized by mean subtraction. Pathway analysis and network analysis were performed using pairwise Student’s t-test to determine CSFR1-regulated sites after treatment by pexidartinib. Proteins carrying significantly regulated phosphorylation sites were subsequently used as input for interaction and pathway analyses using DAVID, KEGG and STRING databases.

Pyrosequencing

Pyrosequecing experiments were performed at Zymo Research. Detail protocol included in supplemental materials.

RESULTS

CSF1R is expressed in peripheral T-cell lymphomas

To examine CSF1R expression in peripheral T-cell lymphomas (PTCL) and cutaneous T-cell lymphomas (CTCL), patient biopsies were analyzed by immunohistochemical staining (Figure 1A–C and supplementary figure 1A–D). CSF1R expression was most prevalent in cutaneous T-cell lymphomas, as ≥30% of tumor cells expressed CSF1R in 52% of the cases examined (n = 54). CSF1R expression was variable, being observed in 5–99% of tumor cells (mean 54%) among the CTCL cases examined (Figure 1B). Aberrant expression of CSF1R was also detected in different subtypes of peripheral T-cell lymphomas, including anaplastic large cell lymphomas (ALCL, 46%; n=11), extranodal NK/T cell lymphomas (ENKTCL, 60%; n = 6), PTCL, non-otherwise specified (PTCL, NOS, 25%; n=59) and angioimmunoblastic T-cell lymphomas (AITL, 7%; n=33) (Figures 1A–C). The number of tumor cells with aberrant expression of CSF1R was variable among PTCL cases, ranging from 10% to 95% (average 16%). As anticipated, CSF1R was localized within the cytoplasm and membrane of TCL cells. Consistent with these findings, CSF1R was detected in protein extracts from T-cell lymphoma lines (Figure 1D), and was expressed at the cell surface (supplementary figure 2A). In order to evaluate whether aberrant epigenetic regulation at the *CSF1R* promoter may explain its aberrant expression in T-cell lymphomas, as observed in classic Hodgkin lymphoma, the presence of non-canonical and canonical *CSF1R* transcripts(39) was evaluated among different T-cell lymphoma lines. These experiments demonstrated that canonical and non-canonical *CSF1R* transcripts were present in cells that expressed CSF1R, but were largely undetectable in cells that did not express CSF1R (supplementary figure 2B). Loss of the epigenetic repressor CBFA2T3 in classic Hodgkin lymphoma is associated with decreased methylation at regulatory sequences in *CSF1R*, and increased CSF1R expression. In order to evaluate the mechanism for deregulated CSF1R expression in T-cell lymphomas, assessment of CBFA2T3 expression was performed on different subtypes of T-cell lymphoma cases and cell lines (supplementary figure 2C). Evaluation of CBFA2T3 expression in ALCL, PTCL, NOS and ENKTCL cases that harbor aberrant expression of CSF1R, revealed that CBFA2T3 is constitutively expressed in these tumors (supplementary figure 2E–G). In contrast, decreased expression of CBFA2T3 was observed in a large proportion of CTCL cases (69%, n = 29). Importantly, a large proportion of cases with decreased CBFA2T3 expression aberrantly expressed CSF1R (70%, supplementary figure 2G). Consistent with this, expression of non-canonical CSF1R transcripts were detectable in CTCL cases with low or absent CBFA2T3 expression (supplementary figure 2C). To further evaluate the role of CBFA2T3 in CSF1R expression, CBFA2T3 was knocked down in T8ML1 cells. CBFA2T3 knock-down was associated with a 3-fold increase in non-canonical CSF1R transcripts, in comparison with scramble shRNA (supplementary figure 2D). To further analyze the potential epigenetic regulation of *CSF1R* transcription, transcripts were quantified after treatment with combinations of hypomethylating agents (decitabine or azacytadine) and a histone deacetylase inhibitor

(belinostat). Treatment with these agents significantly increased non-canonical and canonical transcripts in TCL lines, suggesting that CSF1R expression in TCL may be epigenetically regulated (supplementary figure 3A and B). In addition, pyrosequencing of the alternative CSF1R promoter(39) demonstrated that TCL lines with high-expression of non-canonical transcripts feature 20-fold decrease in methylation at two CpG conserved residues, in comparison with TCL cell lines that feature low-levels of non-canonical transcripts (supplementary figure 3D). These findings demonstrate that CSF1R is aberrantly expressed, to varying degrees, in multiple TCL subsets, and its expression is likely epigenetically regulated. To evaluate whether CSF1R is activated in these cells, CSF1R phosphorylation was analyzed. CSF1R phosphorylation was detected among the T-cell lymphoma lines evaluated, suggesting that CSF1R is activated in a subset of T-cell lymphoma lines (Figure 1E and supplementary figure 3C). In order to investigate if activation of CSF1R can occur secondary to autocrine secretion/activation of CSF1/CSF1R, lymphoma-derived secretion of CSF1 was tested in TCL supernatants by ELISA. Secreted CSF1 was detected at different concentrations from the media of cultured T-cell lymphoma lines (Figure 1F). Similarly, *CSF1* mRNA was detected from tested TCL lines, and was absent in lines that did not secrete CSF1 (supplementary figure 3F). Importantly, the provision of exogenous CSF1 to TCL cells that do not produce CSF1 led to CSF1R activation in a time-dependent manner (supplementary figure 3G). Overall, these findings demonstrate that CSF1R and CSF1 are expressed in TCL, and further, CSF1R activation may occur in an autocrine- or paracrine-dependent manner.

CSF1R activity promote the growth of T-cell lymphomas in-vitro

Having established the expression and activation of CSF1R in TCL, we adopted a loss-of-function strategy to address its potential oncogenic role in these TCL using complementary molecular and pharmacologic approaches. We first used a clinically available and rationally designed tyrosine kinase inhibitor that is selective for CSF1R (Pexidartinib, PLX3397) (25,49). In order to confirm CSF1R inhibition upon pexidartinib treatment, TCL cells with autocrine-activation of CSF1R were treated with pexidartinib. A marked decrease in CSF1R phosphorylation was observed upon treatment with pexidartinib (Figure 2A, supplementary figure 4A). Importantly, pexidartinib did not show any effect on the phosphorylation levels of the oncogenic kinase NPM-ALK which is expressed in a portion of the TCL cells evaluated (supplementary figure 4B). In addition, a dose-dependent decrease in proliferation was observed with exposure to pexidartinib (Figure 2B and supplementary figure 4D–E), however these effects were not observed in TCL cells that do not express CSF1R, supporting the relative selectivity of this FDA-approved agent (supplementary figure 4C). Consistent with these findings, treatment with pexidartinib was associated with increased apoptosis of TCL cells, as demonstrated by phosphatidylserine exposure (Figure 2C–E), PARP cleavage and Caspase 3 cleavage (Figure 2F and supplementary figure 4F). To further address the role of CSF1R in T-cell lymphoma growth, and exclude the possibility of off-target effects with a TKI, doxycycline-inducible stable expression of *CSF1R*-targeting shRNA were successfully generated in T-cell lymphoma-derived lines. To exclude shRNA ‘off-target’ effects, two different shRNA constructs were generated (Figure 3A and B). Following CSF1R knock-down, the viability of T-cell lymphoma lines was measured at 24hrs intervals for up to 72hrs. CSF1R knockdown led to a significant decrease in viability by 1.5-fold and 1.7-fold

(n=4, p<0.01) in comparison with controls (Figure 3C). To further examine the role of CSF1R during lymphoma growth, colony-formation assays were performed. T-cell lymphoma cells with CSF1R knock-down were cultured in methocult media, and colony formation was assessed after 10 days of culture. CSF1R knockdown led to a 1.5-fold and 2.0-fold reduction in colony formation when compared with non-targeting shRNA (n = 3, p<0.01) (Figure 3D and E). Collectively, these findings indicate that CSF1/CSF1R-dependent signaling promotes TCL growth and survival.

Activation of CSF1R is associated with phosphorylation of different signaling pathways

Physiological engagement and activation of CSF1R results in downstream phosphorylation-dependent signaling that modifies the survival and differentiation of myeloid lineage cells(33,34). However, the downstream signals that are regulated by CSF1R activation in most non-myeloid lineage cells are not known. In order to characterize the signaling pathways that are activated by CSF1R, an unbiased phosphoproteomic approach was performed after inhibition of CSF1R activity with pexidartinib in T-cell lymphoma lines. For this screening, Karpas 299 T-cell lymphoma lines were selected because the secretion of CSF1 ligand together with strong surface expression of CSF1R are present. This screen identified a total of 1936 independent phosphotyrosine peptides corresponding to 1123 proteins. In addition, a combined set of 8045 independent phophoserine/phosphothreonine peptides, corresponding to a total number of 3136 proteins were also identified in the screen (supplementary table 1 and 2). A significant reduction in CSF1R auto-phosphorylated peptides was observed in pexidartinib treated cells, further validating this approach (table 1, supplementary figure 5A and supplementary table 3). Hierarchical clustering was performed from three technical replicates, demonstrating that pexidartinib-treated cells formed a distinct cluster (Figure 4A and supplementary figure 5B), encompassing a total of 551 unique proteins with significant modifications in phosphorylated peptides. Out of those phosphorylated peptides, 451 were modifications in serine residues, 122 tyrosine residues and 113 threonine resides (supplementary table 3). Signaling pathway analysis of these changes following CSF1R inhibition was performed with Kyoto Encyclopedia of Genes and Genomes (KEGG online software), and was consistent with differential phosphorylation of PI3K/AKT-regulated signaling (Supplementary Table 1, Figure 4B). Also, modifications in proteins that participate in cellular processes, including metabolism, cell cycle progression and actin-cytoskeleton dynamics were also identified (Figure 4B, supplementary table 4 and supplementary figure 5C). To further explore the signaling pathways that are activated downstream of CSF1R signaling, an unbiased gene expression profile array was performed upon CSF1R inhibition with pexidartinib. The expression of 217 genes was significantly altered upon CSF1R inhibition with pexidartinib (n=3, p<0.01; Figure 4C). Importantly, inhibition of CSF1R was associated with changes in the expression of genes that are involved in cytokine (JAK/STAT) signaling (Figure 4D). Similarly, the phosphoproteomic screening demonstrated differential phosphorylation of proteins that are involved in JAK/STAT signaling, including STAT1, STAT3, STAT5 and SOS2 (supplementary table 2). Because the T-cell line used in the screen harbors the oncogenic NPM-ALK fusion, cells treated with the ALK inhibitor crizotinib were included as a control. In comparison with ALK inhibition, 46% (n = 154 genes) of the changes in gene expression observed in

pexidartinib-treated cells were specific for pexidartinib (Figure 4E), and expression of 63 genes were modified by treatment with either pexidartinib or crizotinib (Figure 4E).

Activation of CSF1R is associated with AKT and mTORC1 activation

As the phosphoproteomic screen implicated the PI3K/AKT/mTOR pathway (Table 1), and having established a functional role for CSF1R activation during T-cell lymphoma growth, the PI3K/AKT/mTOR pathway was examined further. The PI3K regulatory subunit (p85) binds phosphorylated tyrosine(s) within the CSF1R cytoplasmic tail via its SH2 domain, and is required for downstream mTOR activation in macrophages(15), demonstrating a PI3K-dependent link between CSF1R and mTOR activation. Phosphorylation-dependent activation of AKT (PKB) is required for activation of the mTOR/raptor complex (mTORC1), and plays a critical role in tumor growth and survival(50,51), including T-cell lymphomas(52,53). Further analysis of the phosphoproteomic analysis, with less stringent statistical criteria and at least an average of 1.5 fold-change, revealed modifications in several proteins within the PI3K/AKT/mTOR pathway (Figure 5A). Similarly, a targeted approach for quantitative gene expression, demonstrated that several members of the PI3K/AKT/mTOR axis were differentially expressed upon CSF1R activation (Figure 5B and supplementary figure 6B). In order to examine the extent to which CSF1R activation promotes AKT-signaling, AKT phosphorylation was analyzed upon CSF1R inhibition. Phosphorylation of AKT (S473) was decreased in a time-dependent manner upon inhibition of CSF1R (Figure 5C and supplementary figure 6A). However, phosphorylation of AKT (T308) was detected at very low levels, and precluded any further analysis of differential phosphorylation in the conditions tested (data not shown). Phosphorylation of extracellular signal-regulated kinase (ERK) is regulated downstream of CSF1R in myeloid lineages, and contributes to mTORC1 activation independently of PI3K (54). Therefore, phosphorylation of ERK was evaluated downstream of CSF1R activation. No changes in phosphorylated ERK, or total ERK levels were detected downstream of CSF1R inhibition (pexidartinib), suggesting that CSF1R activation does not contribute to ERK phosphorylation in T-cell lymphomas (Figure 5C). In order to investigate the role of PI3K in CSF1R-dependent AKT phosphorylation, T-cell lymphoma lines were cultured with a PI3Kγ/δ inhibitor, tenalisib (RP6530). PI3K inhibition was associated with diminished AKT phosphorylation, with no changes in the total levels of AKT (Figure 5D). Similarly, cells were cultured with CSF1 in the presence or absence of tenalisib. CSF1 led to CSF1R activation and AKT (S473) phosphorylation (Figure 5E). However, PI3K inhibition with tenalisib abrogated AKT phosphorylation (Figure 5E), suggesting that CSF1R-mediated AKT (S473) phosphorylation is PI3K-dependent. Phosphorylation of AKT at S473 is required for optimal AKT activity(55,56), leading to mTORC1 activation and phosphorylation of its substrates, including p70S6K and 4EBP1, both of which promote tumor growth and proliferation(53,57,58). To further explore the link between CSF1R and mTORC1 activation, p70S6K and 4EBP1 phosphorylation were evaluated upon CSF1R activation. CSF1R activation led to a significant increase in 4EBP1 and p70S6K phosphorylation (Figure 5F and G), and phosphorylation of these mTORC1 substrates was inhibited up CSF1R inhibition with pexidartinib (Figure 5F). Overall, these findings further support a role for CSF1R in T-cell lymphomas.

Activation of CSF1R promotes PTCL growth in-vivo

In order to further address the therapeutic relevance of these findings, the growth of T-cell lymphoma xenografts was evaluated upon CSF1R inhibition with pexidartinib. Murine CSF1 does not bind human CSF1R(48,59); therefore, the autocrine-dependent CSF1R activation was evaluated in Karpas 299 xenografts generated in NSG mice. Tumor-bearing mice were treated with sham- or pexidartinib-containing chow, and no treatment-related toxicity was appreciated. An approximately 50% reduction in tumor growth was observed in pexidartinib-treated mice ($n=24$, $p<0.05$; Figure 6A and B), and increased apoptosis was observed from protein extracts of tumors treated with pexidartinib (Figure 6C). Phosphorylation of CSF1R (Y699) and p70S6K (T389) were examined as pharmacodynamic biomarkers using protein extracts from these xenografts, and a significant reduction in phosphorylation was observed in pexidartinib-treated mice (Figure 6D). In similarly designed experiments, SUP-M2 cells (that require exogenous CSF1) were utilized, and xenografts generated in immunodeficient mice that either transgenically express human CSF1(48) or in non-CSF1 expressing controls. An approximately 3-fold increase in tumor volume was observed in CSF1 producing mice compared with control mice ($n=32$, $p<0.001$; Figure 6E and F). Importantly, tumor growth was inhibited in pexidartinib-treated CSF1 transgenic mice ($n=15$, $p<0.001$; Figure 6E and F). However, no significant change in tumor growth was observed in the control mice treated with pexidartinib (Figure 6E and F). Overall, these findings demonstrate that activation of CSF1R, in either an autocrine- or paracrine-dependent manner, promotes T-cell lymphoma growth, and further supports CSF1R as a rational therapeutic target in these lymphomas (supplementary figure 7).

Discussion

CSF1R plays an important role in regulating the homeostatic survival of tumor-associated macrophages (TAM), which promote tumorigenesis in many human cancers, including non-Hodgkin lymphomas(3,12,13,60). Therefore, CSF1R antagonism has emerged as an attractive therapeutic strategy in many cancers, and is currently being examined in clinical trials using both TKI- and monoclonal antibody-based strategies. While CSF1R expression is generally thought to be restricted to myeloid-lineage cells, more recent studies have convincingly demonstrated its aberrant expression on non-myeloid lineage cells, including malignant B cells and classical Hodgkin's lymphoma (cHL)(12,38,39). Given the importance of CSF1R-expressing macrophages in T-cell lymphoma pathogenesis, we investigated the extent to which CSF1R may be expressed by malignant T-cells, as prior studies had suggested that CSF1R may be expressed in anaplastic large cell lymphomas (ALCL)(12,39,61). In a large cohort of primary TCL specimens, CSF1R was prevalent in the most common TCL subtypes (e.g. PTCL, NOS), and was also observed in ALCL and cHL, as previously reported. Our findings demonstrate that CSF1R, while of little value as a diagnostic biomarker due to its expression across TCL subtypes, is an attractive therapeutic target (supplementary figure 7).

Elegant studies performed in cHL demonstrated that derepression of a long-tandem repeat (LTR) generates non-canonical CSF1R transcripts. LTR's are commonly silenced epigenetically by methylation, and expression of the *CSF1R* gene is regulated by

methylation-dependent mechanisms within the promoter and upstream LTR region during normal hematopoiesis(39,62). The loss of expression of the ETO family member CBFA2T3 in Hodgkin's lymphoma cells is associated with decreased methylation within the *CSF1R* LTR, explaining the aberrant CSF1R expression observed in these cells(39). While non-canonical transcripts were detectable in cell lines, we were unable to detect these transcripts in primary PTCL, NOS specimens (data not shown). Consistent with these findings, the transcriptional repressor CBFA2T3, which is characteristically lost in CSF1R-expressing cHL, was expressed in the TCL we examined, with the exception of CTCL(39) (supplementary figure 2E). Epigenetic dysregulation is a recurring theme in many TCL(3), and the increased *CSF1R* transcription we observed upon treatment with either hypomethylating agents or HDAC inhibitors may be consistent with an epigenetic mechanism contributing to the aberrant CSF1R expression we observed in CBFA2T3-expressing cells. Previous genomic and next-generation sequencing studies in both cutaneous and peripheral T-cell lymphomas(63–65) did not identify mutations or alterations in the CSF1R gene, suggesting that aberrant CSF1R expression in T-cell lymphomas is primarily due to its epigenetic dysregulation. Collectively, these results suggest that additional epigenetic mechanisms, independent from CBFA2T3 loss, may explain CSF1R expression in the PTCL. The extent to which these therapeutic agents may select for CSF1R-expressing clones, while an interesting question, is unknown.

Lymphoma-associated macrophages (LAM) are abundant constituents of the microenvironment in the T-cell lymphomas, where they promote tumor growth and suppress host anti-tumor immunity(12). Our findings demonstrate that CSF1 is secreted by malignant T-cells, and may represent an important mechanism by which LAM are recruited and retained in these lymphomas. Within the TME, LAM directly promote the growth and survival of malignant T-cells by providing both cell-surface ligands and cytokines (3). Therefore, the observation that paracrine-activation of CSF1R in T-cell lymphoma lines was associated with increased tumor growth, suggests that CSF1 secretion from cells within the tumor microenvironment, including LAM, promote T-cell lymphoma growth and survival. However, our findings also show that autocrine-activation of CSF1R promotes lymphoma growth in the absence of exogenous CSF1. CSF1 is post-translationally modified and often retained within the extracellular matrix, and may be difficult to detect in plasma(66,67), and could explain why CSF1 was rarely detected in plasma from TCL patients (data not shown). Future studies will be needed in a larger cohort of patients to examine the extent to which CSF1R expression is associated with disease natural history or response to therapy.

The phosphoproteomic and gene expression profile demonstrate activation of conserved signaling pathways downstream of CSF1R/CSF1, including those that have been previously implicated in lymphoma progression. The mammalian target of rapamycin (mTOR) is a downstream target of PI3K/AKT and is the catalytic subunit of two distinct complexes, mTORC1 and mTORC2, both of which are distinguishable by their association with regulatory proteins, including Raptor and Rictor, respectively. In conventional T-cells, mTOR activation is regulated by antigen, costimulatory, and cytokine receptor signaling(3), and regulates T-cell survival, differentiation, metabolism and effector functions(68–73). Consistent with its role in normal T-cell biology and oncogenic role in other malignancies, it is not surprising that constitutive mTOR activation has been implicated in T-cell

lymphomas(52). Importantly, gene-expression profiling studies have identified a cluster of PTCL cases characterized by poor clinical outcomes and dysregulation of Pi3K-mTOR signaling(7,63). Furthermore, the response rate observed (44%) with the mTORC1 inhibitor everolimus(52) approximates that observed with the PI3K inhibitors duvelisib and tenalisib(74). Nonetheless, additional signaling pathways may also contribute to the CSF1R-dependent oncogenic effects observed in T-cell lymphomas. Conversely, multiple CSF1R-independent mechanisms may promote mTOR activation in the TCL, including antigen-receptor signaling (6,75), cytokine signaling (71,75), ICOS activation in T_{FH}-derived TCL, and the genetic landscape (including PTEN deletion)(3).

The transcription and translation of regulatory cytokines and transcription factors may be temporally and spatially segregated in normal T-cells, as the mRNA translation machinery is largely suppressed in resting T-cells. However, upon activation, mRNA translation is unleashed in response to mTORC1-dependent increases in translation initiation and 5'-cap dependent translation(76). Consequently, the translation of relevant cytokines (e.g. IL-4), oncogenes (e.g. c-Myc), and transcription factors (e.g. GATA-3) that have been previously implicated in TCL pathogenesis may be regulated in a mTORC1-dependent manner (6,58,73,76). Therefore, a proteomic approach, as opposed to the gene expression profiling approach we adopted here, may provide a more comprehensive assessment of CSF1R- and mTOR-dependent proteins in the TCL. For example, mTORC1 has been previously implicated in the translational regulation of GATA-3(6,73), a transcription factor that was recently found to identify a distinct subset of PTCL, NOS that was enriched for mTOR-dependent genes(7,44) and associated with chemotherapy resistance and poor outcomes(6). As mTOR plays a central role in regulating T-cell metabolism, the role of CSF1R (and PI3K/AKT/mTOR) in regulating metabolism of malignant T-cells warrants further study and may have significant therapeutic implications(77–79).

In summary, CSF1R is aberrantly expressed in cutaneous and peripheral T-cell lymphomas and is activated by CSF1 in an autocrine- or paracrine-dependent manner. CSF1R activations leads to AKT phosphorylation in a PI3K-dependent manner, promoting the growth and survival of malignant T cells. Consequently, selective CSF1R inhibitors (e.g. pexidartinib) may have a novel dual mechanism of action in these lymphomas – depleting CSF1R-expressing lymphoma-associated macrophages on the one hand, and inhibiting cell-autonomous CSF1R signaling in malignant T cells on the other (supplementary Figure 7).

Supplementary Material

Refer to Web version on PubMed Central for supplementary material.

Acknowledgements

Craig Johnson and Dr. Chris Krebs from the University of Michigan, Biomedical Research Core Facilities DNA Sequencing Core and Microarray. Gary Shangguan for technical assistance. This work was supported by grants from the NIH/National Cancer Institute K08-CA218460 (CMZ), LLS-TRP grant (#R6503-16), the 2017 AACR-Bayer Innovation and Discovery Grant (Grant Number 17-80-44-WILC), ACS (129084-RSG-16-045-01-LIB) and R37-CA233476 (RW), and by internal funds from the University of Michigan department of pathology (NB). Research reported in this manuscript was supported by the National Cancer Institute of the National Institutes of Health under award number P30CA046592.

REFERENCES

1. Ellin F, Landstrom J, Jerkeman M, Relander T. Real-world data on prognostic factors and treatment in peripheral T-cell lymphomas: a study from the Swedish Lymphoma Registry. Blood 2014;124(10):1570–7 doi 10.1182/blood-2014-04-573089. [PubMed: 25006130]
2. Ondrejka SL, Hsi ED. T-cell Lymphomas: Updates in Biology and Diagnosis. Surg Pathol Clin 2016;9(1):131–41 doi 10.1016/j.path.2015.11.002. [PubMed: 26940273]
3. Wilcox RA. A three-signal model of T-cell lymphoma pathogenesis. Am J Hematol 2016;91(1): 113–22 doi 10.1002/ajh.24203. [PubMed: 26408334]
4. Zhang JY, Briski R, Devata S, Kaminski MS, Phillips TJ, Mayer TL, et al. Survival following salvage therapy for primary refractory peripheral T-cell lymphomas (PTCL). Am J Hematol 2018;93(3):394–400 doi 10.1002/ajh.24992. [PubMed: 29194714]
5. Briski R, Feldman AL, Bailey NG, Lim MS, Ristow K, Habermann TM, et al. Survival in patients with limited-stage peripheral T-cell lymphomas. Leukemia & lymphoma 2015;56(6):1665–70 doi 10.3109/10428194.2014.963078. [PubMed: 25248884]
6. Wang T, Lu Y, Polk A, Chowdhury P, Zamalloa CM, Fujiwara H, et al. T-cell Receptor Signaling Activates an ITK/NF-kappaB/GATA-3 axis in T-cell Lymphomas Facilitating Resistance to Chemotherapy. Clin Cancer Res 2017;23(10):2506–15 doi 10.1158/1078-0432.CCR-16-1996. [PubMed: 27780854]
7. Iqbal J, Wright G, Wang C, Rosenwald A, Gascoyne RD, Weisenburger DD, et al. Gene expression signatures delineate biological and prognostic subgroups in peripheral T-cell lymphoma. Blood 2014;123(19):2915–23 doi 10.1182/blood-2013-11-536359. [PubMed: 24632715]
8. Wilcox RA, Sun DX, Novak A, Dogan A, Ansell SM, Feldman AL. Inhibition of Syk protein tyrosine kinase induces apoptosis and blocks proliferation in T-cell non-Hodgkin's lymphoma cell lines. Leukemia 2010;24(1):229–32 doi leu2009198 [pii] 10.1038/leu.2009.198. [PubMed: 19776763]
9. Wada DA, Wilcox RA, Weenig RH, Gibson LE. Paucity of intraepidermal FoxP3-positive T cells in cutaneous T-cell lymphoma in contrast with spongiotic and lichenoid dermatitis. J Cutan Pathol 2010;37(5):535–41 doi 10.1111/j.1600-0560.2009.01381.xCUP1381 [pii]. [PubMed: 19674197]
10. Wilcox RA, Wada DA, Ziesmer SC, Elsawa SF, Comfere NI, Dietz AB, et al. Monocytes promote tumor cell survival in T-cell lymphoproliferative disorders and are impaired in their ability to differentiate into mature dendritic cells. Blood 2009;114(14):2936–44. [PubMed: 19671921]
11. Berger CL, Hanlon D, Kanada D, Dhodapkar M, Lombillo V, Wang N, et al. The growth of cutaneous T-cell lymphoma is stimulated by immature dendritic cells. Blood 2002;99(8):2929–39. [PubMed: 11929784]
12. Martin-Moreno AM, Roncador G, Maestre L, Mata E, Jimenez S, Martinez-Torrecuadrada JL, et al. CSF1R Protein Expression in Reactive Lymphoid Tissues and Lymphoma: Its Relevance in Classical Hodgkin Lymphoma. PLoS One 2015;10(6):e0125203 doi 10.1371/journal.pone. 0125203. [PubMed: 26066800]
13. Polk A, Lu Y, Wang T, Seymour E, Bailey NG, Singer JW, et al. Colony-Stimulating Factor-1 Receptor Is Required for Nurse-like Cell Survival in Chronic Lymphocytic Leukemia. Clin Cancer Res 2016;22(24):6118–28 doi 10.1158/1078-0432.CCR-15-3099. [PubMed: 27334834]
14. Chang M, Hamilton JA, Scholz GM, Masendycz P, Macaulay SL, Elsegood CL. Phosphatidylinostitol-3 kinase and phospholipase C enhance CSF-1-dependent macrophage survival by controlling glucose uptake. Cell Signal 2009;21(9):1361–9 doi 10.1016/j.cellsig. 2009.04.003. [PubMed: 19376223]
15. Munugalavadla V, Borneo J, Ingram DA, Kapur R. p85alpha subunit of class IA PI-3 kinase is crucial for macrophage growth and migration. Blood 2005;106(1):103–9 doi 10.1182/ blood-2004-10-4041. [PubMed: 15769893]
16. Dovas A, Gevrey JC, Grossi A, Park H, Abou-Kheir W, Cox D. Regulation of podosome dynamics by WASp phosphorylation: implication in matrix degradation and chemotaxis in macrophages. J Cell Sci 2009;122(Pt 21):3873–82 doi 10.1242/jcs.051755. [PubMed: 19808890]
17. Byrne PV, Guilbert LJ, Stanley ER. Distribution of cells bearing receptors for a colony-stimulating factor (CSF-1) in murine tissues. J Cell Biol 1981;91(3 Pt 1):848–53. [PubMed: 6276411]

18. Wang Y, Szretter KJ, Vermi W, Gilfillan S, Rossini C, Cella M, et al. IL-34 is a tissue-restricted ligand of CSF1R required for the development of Langerhans cells and microglia. Nature immunology 2012;13(8):753–60 doi 10.1038/ni.2360. [PubMed: 22729249]
19. Kodama H, Nose M, Niida S, Yamasaki A. Essential role of macrophage colony-stimulating factor in the osteoclast differentiation supported by stromal cells. J Exp Med 1991;173(5):1291–4. [PubMed: 2022928]
20. Richardsen E, Uglehus RD, Johnsen SH, Busund LT. Macrophage-colony stimulating factor (CSF1) predicts breast cancer progression and mortality. Anticancer research 2015;35(2):865–74. [PubMed: 25667468]
21. Huynh D, Dai XM, Nandi S, Lightowler S, Trivett M, Chan CK, et al. Colony stimulating factor-1 dependence of paneth cell development in the mouse small intestine. Gastroenterology 2009;137(1):136–44, 44 e1–3 doi 10.1053/j.gastro.2009.03.004. [PubMed: 19303020]
22. Cannarile MA, Weisser M, Jacob W, Jegg AM, Ries CH, Ruttinger D. Colony-stimulating factor 1 receptor (CSF1R) inhibitors in cancer therapy. J Immunother Cancer 2017;5(1):53 doi 10.1186/s40425-017-0257-y. [PubMed: 28716061]
23. Kacinski BM, Scata KA, Carter D, Yee LD, Sapi E, King BL, et al. FMS (CSF-1 receptor) and CSF-1 transcripts and protein are expressed by human breast carcinomas in vivo and in vitro. Oncogene 1991;6(6):941–52. [PubMed: 1829808]
24. Okugawa Y, Toiyama Y, Ichikawa T, Kawamura M, Yasuda H, Fujikawa H, et al. Colony-stimulating factor-1 and colony-stimulating factor-1 receptor co-expression is associated with disease progression in gastric cancer. Int J Oncol 2018;53(2):737–49 doi 10.3892/ijo.2018.4406. [PubMed: 29767252]
25. Tap WD, Wainberg ZA, Anthony SP, Ibrahim PN, Zhang C, Healey JH, et al. Structure-Guided Blockade of CSF1R Kinase in Tenosynovial Giant-Cell Tumor. N Engl J Med 2015;373(5):428–37 doi 10.1056/NEJMoa1411366. [PubMed: 26222558]
26. Chitu V, Gokhan S, Nandi S, Mehler MF, Stanley ER. Emerging Roles for CSF-1 Receptor and its Ligands in the Nervous System. Trends Neurosci 2016;39(6):378–93 doi 10.1016/j.tins.2016.03.005. [PubMed: 27083478]
27. Tanaka M, Kishi K, McCarron RM, Miyatake T. The generation of macrophages from precursor cells incubated with brain endothelial cells--a release of CSF-1 like factor from endothelial cells. Tohoku J Exp Med 1993;171(3):211–20. [PubMed: 8160177]
28. Guilbert LJ, Stanley ER. Specific interaction of murine colony-stimulating factor with mononuclear phagocytic cells. J Cell Biol 1980;85(1):153–9. [PubMed: 6965942]
29. Nandi S, Gokhan S, Dai XM, Wei S, Enikolopov G, Lin H, et al. The CSF-1 receptor ligands IL-34 and CSF-1 exhibit distinct developmental brain expression patterns and regulate neural progenitor cell maintenance and maturation. Dev Biol 2012;367(2):100–13 doi 10.1016/j.ydbio.2012.03.026. [PubMed: 22542597]
30. Wei S, Nandi S, Chitu V, Yeung YG, Yu W, Huang M, et al. Functional overlap but differential expression of CSF-1 and IL-34 in their CSF-1 receptor-mediated regulation of myeloid cells. Journal of leukocyte biology 2010;88(3):495–505 doi 10.1189/jlb.1209822. [PubMed: 20504948]
31. Noy R, Pollard JW. Tumor-associated macrophages: from mechanisms to therapy. Immunity 2014;41(1):49–61 doi 10.1016/j.immuni.2014.06.010. [PubMed: 25035953]
32. Coussens L, Van Beveren C, Smith D, Chen E, Mitchell RL, Isacke CM, et al. Structural alteration of viral homologue of receptor proto-oncogene fms at carboxyl terminus. Nature 1986;320(6059):277–80 doi 10.1038/320277a0. [PubMed: 2421165]
33. Pixley FJ, Stanley ER. CSF-1 regulation of the wandering macrophage: complexity in action. Trends Cell Biol 2004;14(11):628–38 doi 10.1016/j.tcb.2004.09.016. [PubMed: 15519852]
34. Stanley ER, Chitu V. CSF-1 receptor signaling in myeloid cells. Cold Spring Harbor perspectives in biology 2014;6(6) doi 10.1101/cshperspect.a021857.
35. Wyckoff J, Wang W, Lin EY, Wang Y, Pixley F, Stanley ER, et al. A paracrine loop between tumor cells and macrophages is required for tumor cell migration in mammary tumors. Cancer Res 2004;64(19):7022–9 doi 10.1158/0008-5472.CAN-04-1449. [PubMed: 15466195]
36. Patsialou A, Wang Y, Pignatelli J, Chen X, Entenberg D, Oktay M, et al. Autocrine CSF1R signaling mediates switching between invasion and proliferation downstream of TGFbeta in

claudin-low breast tumor cells. Oncogene 2015;34(21):2721–31 doi 10.1038/onc.2014.226. [PubMed: 25088194]

37. Smith HO, Stephens ND, Qualls CR, Fligelman T, Wang T, Lin CY, et al. The clinical significance of inflammatory cytokines in primary cell culture in endometrial carcinoma. Mol Oncol 2013;7(1): 41–54 doi 10.1016/j.molonc.2012.07.002. [PubMed: 22944067]
38. Ullrich K, Wurster KD, Lamprecht B, Kochert K, Engert A, Dorken B, et al. BAY 43–9006/ Sorafenib blocks CSF1R activity and induces apoptosis in various classical Hodgkin lymphoma cell lines. Br J Haematol 2011;155(3):398–402 doi 10.1111/j.1365-2141.2011.08685.x. [PubMed: 21517818]
39. Lamprecht B, Walter K, Kreher S, Kumar R, Hummel M, Lenze D, et al. Derepression of an endogenous long terminal repeat activates the CSF1R proto-oncogene in human lymphoma. Nat Med 2010;16(5):571–9, 1p following 9 doi 10.1038/nm.2129. [PubMed: 20436485]
40. Skinnider BF, Mak TW. The role of cytokines in classical Hodgkin lymphoma. Blood 2002;99(12): 4283–97 doi 10.1182/blood-2002-01-0099. [PubMed: 12036854]
41. Komohara Y, Noyori O, Saito Y, Takeya H, Baghdadi M, Kitagawa F, et al. Potential anti-lymphoma effect of M-CSFR inhibitor in adult T-cell leukemia/lymphoma. J Clin Exp Hematop 2018;58(4):152–60 doi 10.3960/jslrt.18034. [PubMed: 30541986]
42. Giustini N, Bernthal NM, Bukata SV, Singh AS. Tenosynovial giant cell tumor: case report of a patient effectively treated with pexidartinib (PLX3397) and review of the literature. Clin Sarcoma Res 2018;8:14 doi 10.1186/s13569-018-0101-2. [PubMed: 30002809]
43. Murga-Zamalloa CA, Mendoza-Reinoso V, Sahasrabuddhe AA, Rolland D, Hwang SR, McDonnell SR, et al. NPM-ALK phosphorylates WASp Y102 and contributes to oncogenesis of anaplastic large cell lymphoma. Oncogene 2017;36(15):2085–94 doi 10.1038/onc.2016.366. [PubMed: 27694894]
44. Wang T, Feldman AL, Wada DA, Lu Y, Polk A, Briski R, et al. GATA-3 expression identifies a high-risk subset of PTCL, NOS with distinct molecular and clinical features. Blood 2014;123(19): 3007–15 doi 10.1182/blood-2013-12-544809. [PubMed: 24497534]
45. Zhang Q, Wang H, Kantekure K, Paterson JC, Liu X, Schaffer A, et al. Oncogenic tyrosine kinase NPM-ALK induces expression of the growth-promoting receptor ICOS. Blood 2011;118(11): 3062–71 doi blood-2011–01-332916 [pii] 10.1182/blood-2011-01-332916. [PubMed: 21765024]
46. Rolland D, Basrur V, Conlon K, Wolfe T, Fermin D, Nesvizhskii AI, et al. Global phosphoproteomic profiling reveals distinct signatures in B-cell non-Hodgkin lymphomas. The American journal of pathology 2014;184(5):1331–42 doi 10.1016/j.ajpath.2014.01.036. [PubMed: 24667141]
47. Tyanova S, Temu T, Cox J. The MaxQuant computational platform for mass spectrometry-based shotgun proteomics. Nat Protoc 2016;11(12):2301–19 doi 10.1038/nprot.2016.136. [PubMed: 27809316]
48. Rathinam C, Poueymirou WT, Rojas J, Murphy AJ, Valenzuela DM, Yancopoulos GD, et al. Efficient differentiation and function of human macrophages in humanized CSF-1 mice. Blood 2011;118(11):3119–28 doi blood-2010–12-326926 [pii] 10.1182/blood-2010-12-326926. [PubMed: 21791433]
49. Patwardhan PP, Surriga O, Beckman MJ, de Stanchina E, Dematteo RP, Tap WD, et al. Sustained inhibition of receptor tyrosine kinases and macrophage depletion by PLX3397 and rapamycin as a potential new approach for the treatment of MPNSTs. Clin Cancer Res 2014;20(12):3146–58 doi 10.1158/1078-0432.CCR-13-2576. [PubMed: 24718867]
50. Vadlakonda L, Dash A, Pasupuleti M, Anil Kumar K, Reddanna P. The Paradox of Akt-mTOR Interactions. Front Oncol 2013;3:165 doi 10.3389/fonc.2013.00165. [PubMed: 23802099]
51. Vadlakonda L, Pasupuleti M, Pallu R. Role of PI3K-AKT-mTOR and Wnt Signaling Pathways in Transition of G1-S Phase of Cell Cycle in Cancer Cells. Front Oncol 2013;3:85 doi 10.3389/fonc. 2013.00085. [PubMed: 23596569]
52. Witzig TE, Reeder C, Han JJ, LaPlant B, Stenson M, Tun HW, et al. The mTORC1 inhibitor everolimus has antitumor activity in vitro and produces tumor responses in patients with relapsed T-cell lymphoma. Blood 2015;126(3):328–35 doi 10.1182/blood-2015-02-629543. [PubMed: 25921059]

53. Gupta M, Hendrickson AE, Yun SS, Han JJ, Schneider PA, Koh BD, et al. Dual mTORC1/mTORC2 inhibition diminishes Akt activation and induces Puma-dependent apoptosis in lymphoid malignancies. Blood 2012;119(2):476–87 doi 10.1182/blood-2011-04-346601 [pii]. [PubMed: 22080480]
54. Marzec M, Kasprzycka M, Liu X, El-Salem M, Halasa K, Raghunath PN, et al. Oncogenic tyrosine kinase NPM/ALK induces activation of the rapamycin-sensitive mTOR signaling pathway. Oncogene 2007;26(38):5606–14. [PubMed: 17353907]
55. Sarbassov DD, Guertin DA, Ali SM, Sabatini DM. Phosphorylation and regulation of Akt/PKB by the rictor-mTOR complex. Science 2005;307(5712):1098–101 doi 10.1126/science.1106148. [PubMed: 15718470]
56. Chu N, Salguero AL, Liu AZ, Chen Z, Dempsey DR, Ficarro SB, et al. Akt Kinase Activation Mechanisms Revealed Using Protein Semisynthesis. Cell 2018;174(4):897–907 e14 doi 10.1016/j.cell.2018.07.003. [PubMed: 30078705]
57. Witzig TE, Reeder CB, LaPlant BR, Gupta M, Johnston PB, Micallef IN, et al. A phase II trial of the oral mTOR inhibitor everolimus in relapsed aggressive lymphoma. Leukemia 2011;25(2):341–7 doi 10.1038/leu.2010.226. [PubMed: 21135857]
58. Demosthenous C, Han JJ, Stenson MJ, Maurer MJ, Wellik LE, Link B, et al. Translation initiation complex eIF4F is a therapeutic target for dual mTOR kinase inhibitors in non-Hodgkin lymphoma. Oncotarget 2015;6(11):9488–501. [PubMed: 25839159]
59. Yoshida H, Hayashi S, Kunisada T, Ogawa M, Nishikawa S, Okamura H, et al. The murine mutation osteopetrosis is in the coding region of the macrophage colony stimulating factor gene. Nature 1990;345(6274):442–4 doi 10.1038/345442a0. [PubMed: 2188141]
60. Edwards VD, Sweeney DT, Ho H, Eide CA, Rofelty A, Agarwal A, et al. Targeting of colony-stimulating factor 1 receptor (CSF1R) in the CLL microenvironment yields antineoplastic activity in primary patient samples. Oncotarget 2018;9(37):24576–89 doi 10.18632/oncotarget.25191. [PubMed: 29872489]
61. Mathas S, Kreher S, Meaburn KJ, Johrens K, Lamprecht B, Assaf C, et al. Gene deregulation and spatial genome reorganization near breakpoints prior to formation of translocations in anaplastic large cell lymphoma. Proc Natl Acad Sci U S A 2009;106(14):5831–6 doi 10.1073/pnas.0900912106. [PubMed: 19321746]
62. Tagoh H, Schebesta A, Lefevre P, Wilson N, Hume D, Busslinger M, et al. Epigenetic silencing of the c-fms locus during B-lymphopoiesis occurs in discrete steps and is reversible. EMBO J 2004;23(21):4275–85 doi 10.1038/sj.emboj.7600421. [PubMed: 15483629]
63. Heavican TB, Bouska A, Yu J, Lone W, Amador C, Gong Q, et al. Genetic drivers of oncogenic pathways in molecular subgroups of peripheral T-cell lymphoma. Blood 2019;133(15):1664–76 doi 10.1182/blood-2018-09-872549. [PubMed: 30782609]
64. Kiel MJ, Sahasrabuddhe AA, Rolland DCM, Velusamy T, Chung F, Schaller M, et al. Genomic analyses reveal recurrent mutations in epigenetic modifiers and the JAK-STAT pathway in Sezary syndrome. Nat Commun 2015;6:8470 doi 10.1038/ncomms9470. [PubMed: 26415585]
65. Ng SY, Yoshida N, Christie AL, Ghandi M, Dharia NV, Dempster J, et al. Targetable vulnerabilities in T- and NK-cell lymphomas identified through preclinical models. Nat Commun 2018;9(1):2024 doi 10.1038/s41467-018-04356-9. [PubMed: 29789628]
66. Kremlev SG, Chapoval AI, Evans R. CSF-1 (M-CSF) enhances the inflammatory response of fibronectin-primed macrophages: pathways involved in activation of the cytokine network. Nat Immun 1998;16(5–6):228–43 doi 10.1159/000069449. [PubMed: 11061591]
67. Kremlev SG, Chapoval AI, Evans R. Cytokine release by macrophages after interacting with CSF-1 and extracellular matrix proteins: characteristics of a mouse model of inflammatory responses in vitro. Cell Immunol 1998;185(1):59–64 doi 10.1006/cimm.1998.1276. [PubMed: 9636683]
68. Zeng H, Chi H. mTOR and lymphocyte metabolism. Curr Opin Immunol 2013;25(3):347–55 doi 10.1016/j.coi.2013.05.002. [PubMed: 23722114]
69. Zeng H, Cohen S, Guy C, Shrestha S, Neale G, Brown SA, et al. mTORC1 and mTORC2 Kinase Signaling and Glucose Metabolism Drive Follicular Helper T Cell Differentiation. Immunity 2016;45(3):540–54 doi 10.1016/j.immuni.2016.08.017. [PubMed: 27637146]

70. Zeng H, Yang K, Cloer C, Neale G, Vogel P, Chi H. mTORC1 couples immune signals and metabolic programming to establish T(reg)-cell function. Nature 2013;499(7459):485–90 doi 10.1038/nature12297. [PubMed: 23812589]

71. Ray JP, Staron MM, Shyer JA, Ho PC, Marshall HD, Gray SM, et al. The Interleukin-2-mTORc1 Kinase Axis Defines the Signaling, Differentiation, and Metabolism of T Helper 1 and Follicular B Helper T Cells. Immunity 2015;43(4):690–702 doi 10.1016/j.immuni.2015.08.017. [PubMed: 26410627]

72. Essig K, Hu D, Guimaraes JC, Alterauge D, Edelmann S, Raj T, et al. Roquin Suppresses the PI3K-mTOR Signaling Pathway to Inhibit T Helper Cell Differentiation and Conversion of Treg to Tfr Cells. Immunity 2017;47(6):1067–82 e12 doi 10.1016/j.immuni.2017.11.008. [PubMed: 29246441]

73. Lee K, Gudapati P, Dragovic S, Spencer C, Joyce S, Killeen N, et al. Mammalian target of rapamycin protein complex 2 regulates differentiation of Th1 and Th2 cell subsets via distinct signaling pathways. Immunity 2010;32(6):743–53 doi 10.1016/j.immuni.2010.06.002. [PubMed: 20620941]

74. Horwitz SM, Koch R, Porcu P, Oki Y, Moskowitz A, Perez M, et al. Activity of the PI3K-delta,gamma inhibitor duvelisib in a phase 1 trial and preclinical models of T-cell lymphoma. Blood 2018;131(8):888–98 doi 10.1182/blood-2017-08-802470. [PubMed: 29233821]

75. Ng SY, Brown L, Stevenson K, deSouza T, Aster JC, Louissaint A, Jr., et al. RhoA G17V is sufficient to induce autoimmunity and promotes T-cell lymphomagenesis in mice. Blood 2018;132(9):935–47 doi 10.1182/blood-2017-11-818617. [PubMed: 29769264]

76. Gigoux M, Lovato A, Leconte J, Leung J, Sonenberg N, Suh WK. Inducible costimulator facilitates T-dependent B cell activation by augmenting IL-4 translation. Mol Immunol 2014;59(1):46–54 doi 10.1016/j.molimm.2014.01.008. [PubMed: 24486724]

77. Shukla SK, Purohit V, Mehla K, Gunda V, Chaika NV, Vernucci E, et al. MUC1 and HIF-1alpha Signaling Crosstalk Induces Anabolic Glucose Metabolism to Impart Gemcitabine Resistance to Pancreatic Cancer. Cancer Cell 2017;32(1):71–87 e7 doi 10.1016/j.ccell.2017.06.004. [PubMed: 28697344]

78. Salmond RJ. mTOR Regulation of Glycolytic Metabolism in T Cells. Front Cell Dev Biol 2018;6:122 doi 10.3389/fcell.2018.00122. [PubMed: 30320109]

79. Gupta M, Dillon SR, Ziesmer SC, Feldman AL, Witzig TE, Ansell SM, et al. A proliferation-inducing ligand mediates follicular lymphoma B-cell proliferation and cyclin D1 expression through phosphatidylinositol 3-kinase-regulated mammalian target of rapamycin activation. Blood 2009;113(21):5206–16 doi blood-2008–09-179762 [pii] 10.1182/blood-2008-09-179762. [PubMed: 19321861]

Translational relevance statement

The T-cell lymphomas remain an area of unmet need, as clinical trial participation remains a standard of care in the relapsed/refractory setting, and novel therapeutic strategies are needed. We demonstrate that CSF1R is aberrantly expressed in a significant proportion of peripheral and cutaneous T-cell lymphomas, where it activates PI3K/AKT signaling, and promotes the growth and survival of malignant T cells. Consequently, pexidartinib, a selective CSF1R inhibitor, impaired the growth of CSF1R-expressing T-cell lymphomas. Overall, these findings identify CSF1R as a novel therapeutic target in these lymphomas.

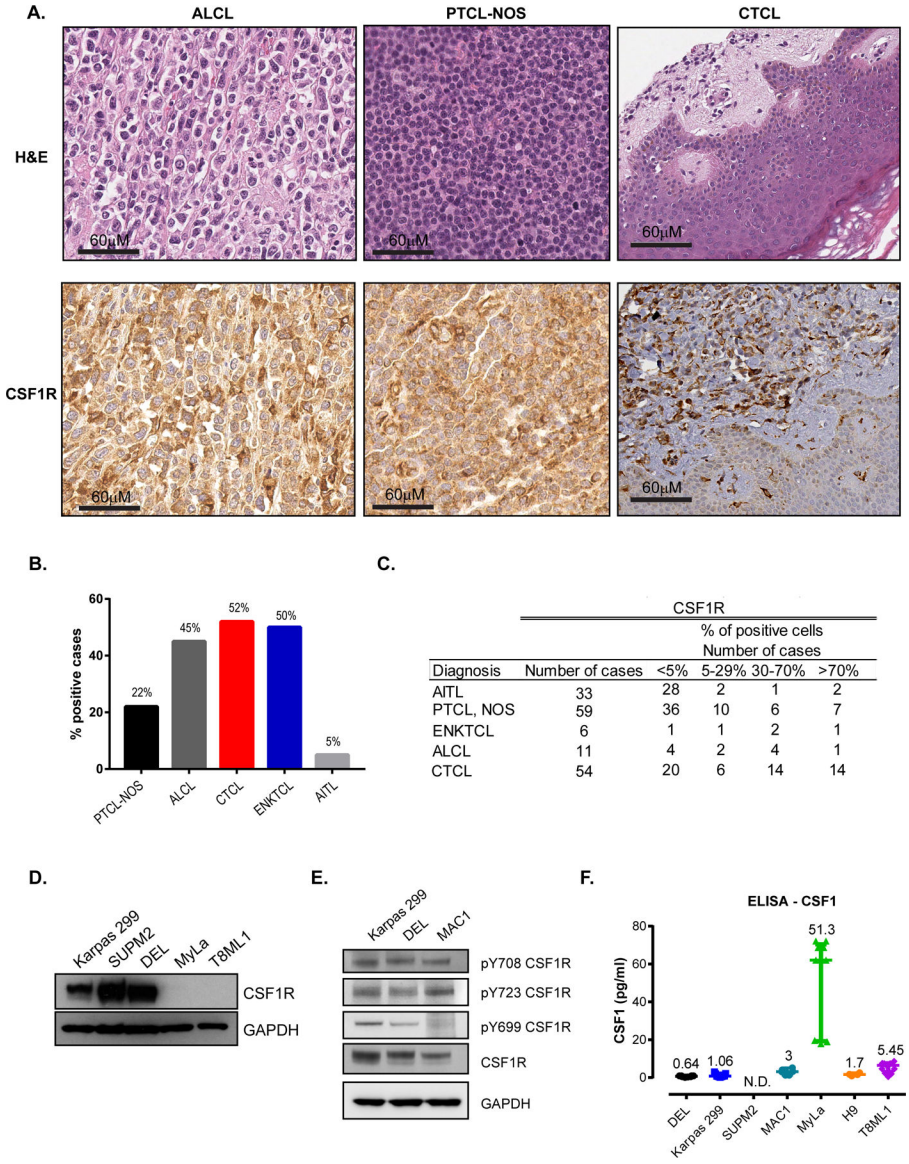

Figure 1.

CSF1R expression in T-cell lymphomas. **A.** Representative photographs of PTCL cases that express CSF1R within the tumor cells (lower panel), and corresponding hematoxylin and eosin (H&E) stain (upper panel). **B.** Comparative analysis CSF1R expression within different subtypes of T-cell lymphomas; (PTCL-NOS n = 59, ALCL n = 11, CTCL n = 31, ENKTCL n = 6 and AITL n = 33). Bars represent the percentage of positive cases for aberrant CSF1R expression within the tumor cells (≥30% positive tumor cells). **C**. Table indicates the number of cells at the indicated percentage intervals that express CSF1R. **D.** Western blot analysis display positive CSF1R protein expression in Karpas 299, SUPM2 and DEL (ALCL), and undetectable expression in MyLa (CTCL) and T8ML1 (PTCL, NOS) lines. **E.** Protein expression of phosphorylated isoforms of CSF1R were detected by western blot analysis in the indicated T-cell lymphoma lines. **F.** Secretion of CSF1 ligand was detected from cell cultured media of the indicated T-cell lymphoma lines by ELISA

immunoassays. Scatter dot plot = mean ± SD. [Anaplastic large cell lymphoma (ALCL), peripheral T-cell lymphoma non-otherwise specified (PTCL-NOS), cutaneous T-cell lymphoma (CTCL), extra-nodal NK-type T-cell lymphoma (ENKTCL) and angioimmunoblastic T-cell lymphoma (AITL)].

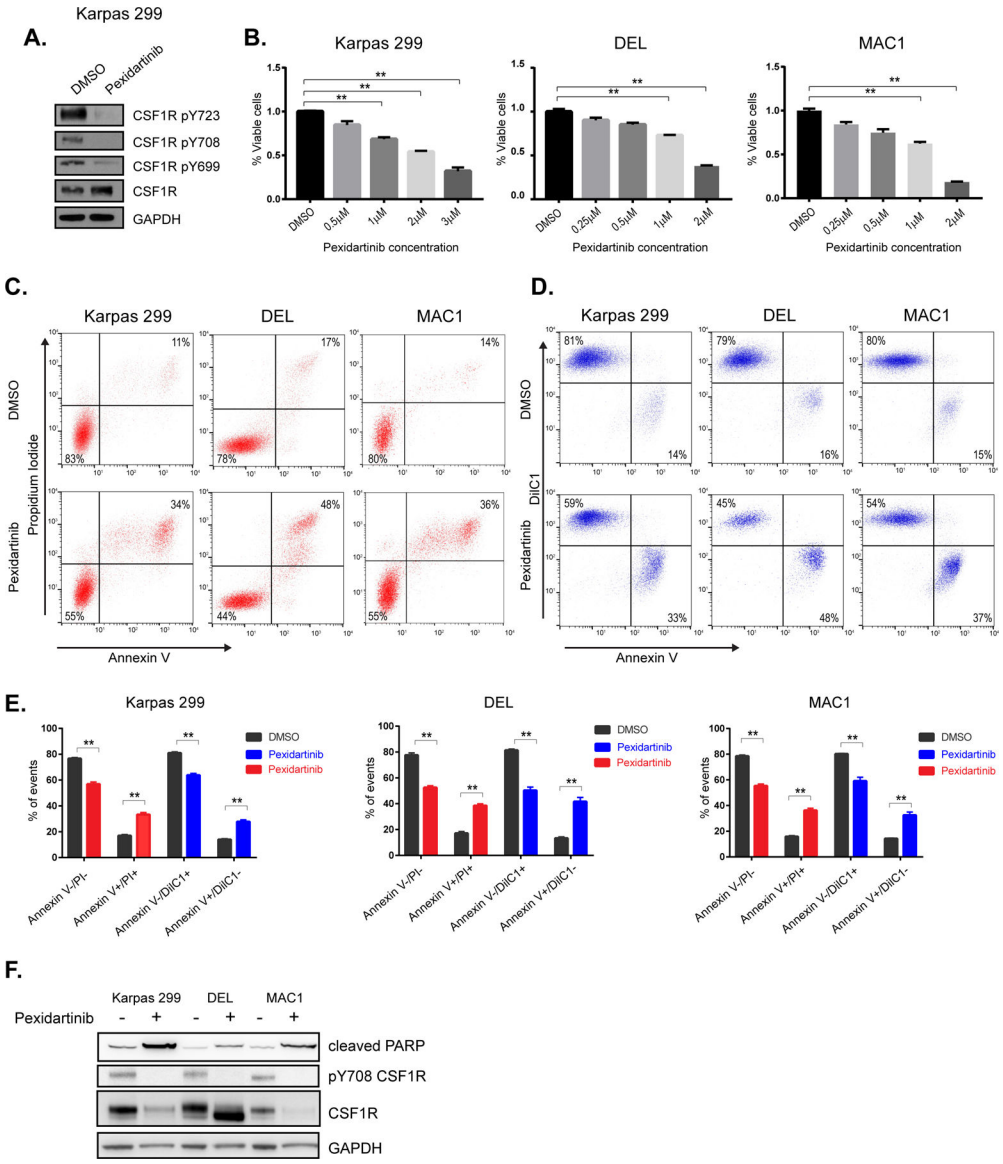

Figure 2.

Pharmacologic CSF1R inhibition with pexidartinib impairs T-cell lymphoma growth and survival. **A.** The expression of phosphorylated Y723-, Y708- and Y699-CSF1R was evaluated upon incubation with 1μM pexidartinib or DMSO vehicle control (time = 30min). **B.** The proliferation of T-cell lymphoma lines was evaluated after 72hrs incubation with indicated doses of pexidartinib. **C.** Annexin V and Propidium Iodide incorporation were measured by flow cytometric analysis upon exposure of pexidartinib (1μM, 72hrs), in order to evaluate the proportion of viable (Annexin V-/Propidium Iodide-) or apoptotic (Annexin V+/Propidium Iodide+) cells. **D.** DilC1 and Annexin V incorporation were measured by flow cytometric analysis upon exposure of pexidartinib (1μM, 72hrs), in order to evaluate the proportion of viable (DilC1+/Annexin V-) or apopototic cells (DilC1-/Annexin V+). **E.** Corresponding column graphs depicts the proportion of viable or apoptotic cells upon exposure to pexidartinib. **F.** Expression of cleaved PARP was evaluated upon exposure to

pexidartinib (1μM, 72hrs), in indicated TCL cells, in order to assess apoptosis. (**A** and **F**) GAPDH as loading control. Figures are representative of at least three independent experiments. (**B** and **D**) Bars = mean ± SEM. **p < 0.01, n = 5.

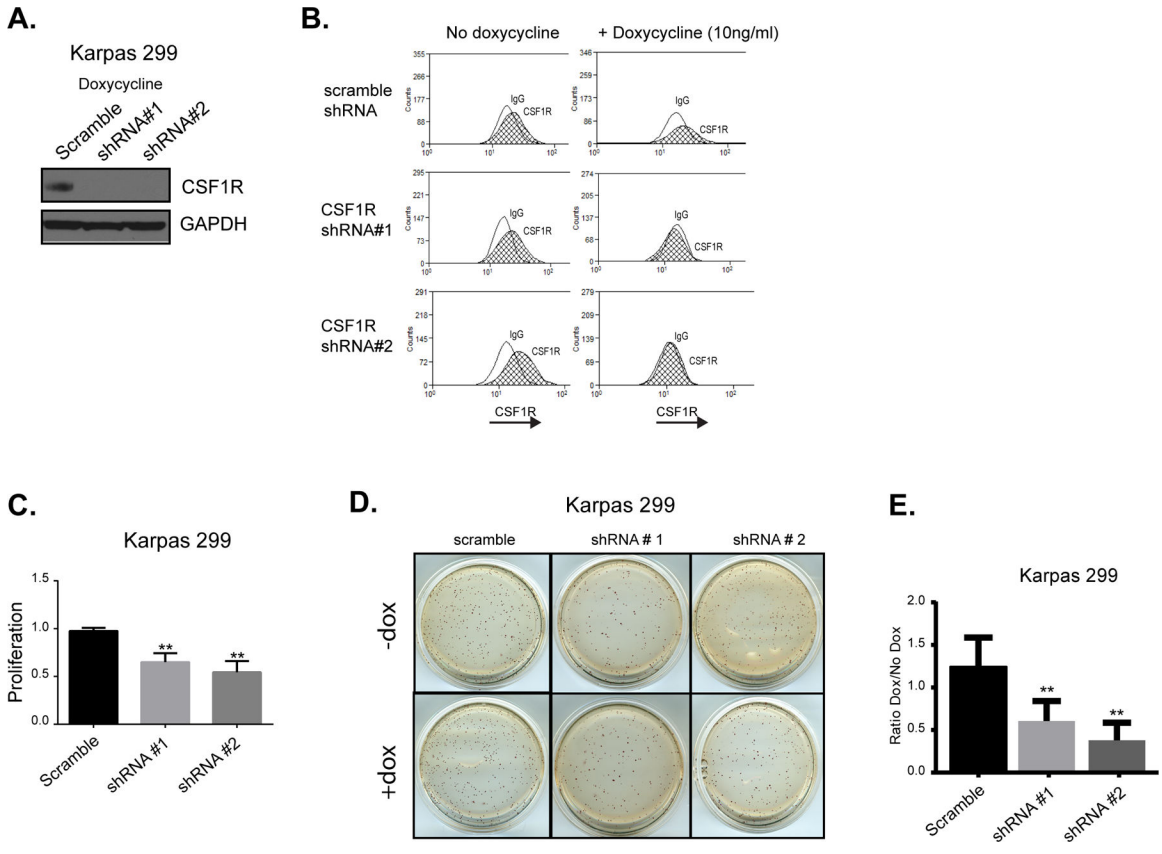

Figure 3.

CSF1R knockdown impairs T-cell lymphoma growth and survival. **A.** The efficiency of CSF1R knock-down upon induction (10ng/ml doxycycline) of two independent CSF1R-specific shRNA sequences (shRNA#1 and shRNA #2) or scramble control, as measured by western blot analysis or flow cytometry testing (**B**). **C.** Proliferation of T-cell lymphoma lines (Karpas 299) was evaluated after 72hrs of CSF1R shRNA or scramble shRNA induction. **D.** Representative pictures of colony formation assays in methocult media (1 week growth) upon induction (+dox) or no induction (-dox) of CSF1R-specific or scramble shRNA. **E.** Bar-graph represents fold-change in the number of colonies when CSF1R-specific or scramble shRNA was induced (Dox) or non-induced (No Dox). Figures are representative of at least three independent experiments. (**A**) GAPDH as loading control. (**C** and **E**) Bars = mean ± SEM. **p < 0.01, n = 5.

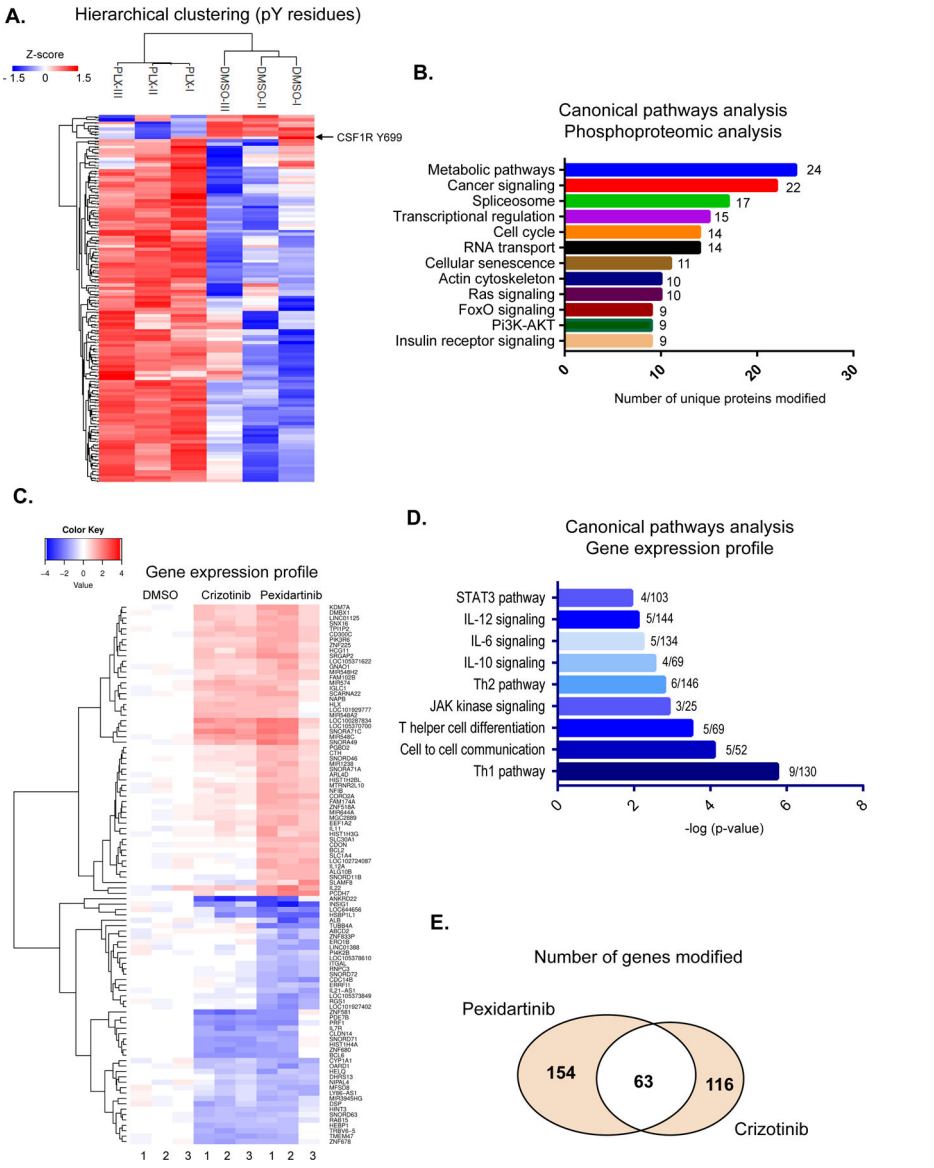

Figure 4.

Phosphoproteomic identification of CSF1R-dependent pathways. (**A–B**) Phosphoproteomic analysis of T-cell lymphoma lines after CSF1R inhibition with pexidartinib. **A.** Clustering of T-cell lymphoma lines (Karpas 299) based on the relative log2 intensities of identified phospho-tyrosine, after treatment with pexidartinib or DMSO vehicle (6hrs). Results represent three independent experiments. **B.** Functional analysis of the most represented canonical pathways based on the differential phosphorylation of proteins after CSF1R inhibition. (**C–E**) Gene expression analysis of T-cell lymphomas after CSF1R inhibition with pexidartinib (24hrs). **C.** Cluster analysis of T-cell lymphoma lines (Karpas 299) based on the average gene-expression after CSF1R inhibition with pexidartinib, NPM-ALK tyrosine kinase inhibition (crizotinib) or DMSO vehicle control. Results represent three independent experiments. **D.** Analysis of the most represented canonical pathways based on the differential gene expression downstream of CSF1R inhibition with pexidartinib **E.** Venn

diagram depicts the number of genes for which its expression is uniquely or commonly modified by CSF1R (pexidartinib) or NPM-ALK (crizotinib) inhibition.

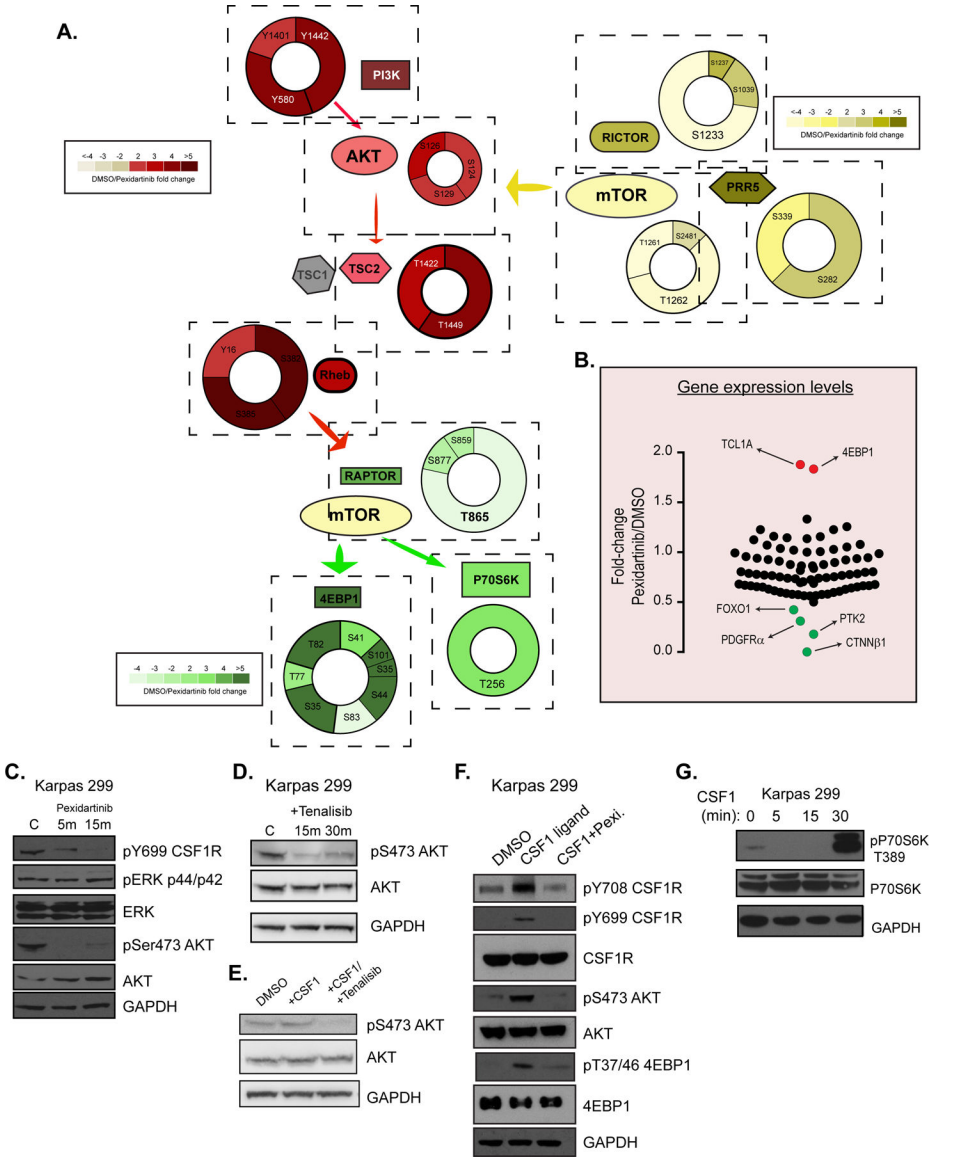

Figure 5.

CSF1R activates PI3K/AKT/mTOR signaling. **A.** Selected proteins that are involved in the PI3K/AKT/mTOR signaling pathway that feature at least an average of 2-fold change in phosphorylation after inhibition of CSF1R. The fold-change degree of quantity change in each direction is indicated by colors. **B.** Expression of selected genes in T-cell lymphoma lines that are components of the PI3K/AKT/mTOR signaling pathway was evaluated by quantitative real-time PCR after inhibition of CSF1R with pexidartinib (24hrs) or vehicle control (DMSO). **C.** Phosphorylation of ERK (p44/p42) and AKT (pSer473) was evaluated by western blot after inhibition of CSF1R (pexidartinib) at indicated times in T-cell lymphoma lines (Karpas 299). **D.** Phosphorylation of AKT (pS473) was evaluated in T-cell lymphoma lines (Karpas 299) downstream of PI3K inhibition with tenalisib at indicated times. **E.** Phosphorylation of CSF1R (pY723) and AKT (pS473) was evaluated in T-cell lymphoma lines (Karpas 299) after incubation with human CSF1 ligand (+CSF1) for 20min.

Dependence of CSF1 signaling on PI3K was as evaluated by concomitant incubation with tenalisib (PI3K inhibitor) (+CSF1/+tenalisib). **F.** Phosphorylation of CSF1R (pY708, pY699), AKT (pS473) and 4EBP1 (pT37/46) was evaluated in T-cell lymphoma lines (Karpas 299) after incubation with human CSF1 ligand for 20min. Specificity of CSF1 ligand activity was evaluated by concomitant incubation with pexidartinib (CSF1 + Pexi). **G.** Phosphorylation of p70S6K (pT389) was evaluated in T-cell lymphoma lines (Karpas 299) upon incubation with human CSF1 ligand at indicated time points. (**C-G**) GAPDH as loading control.

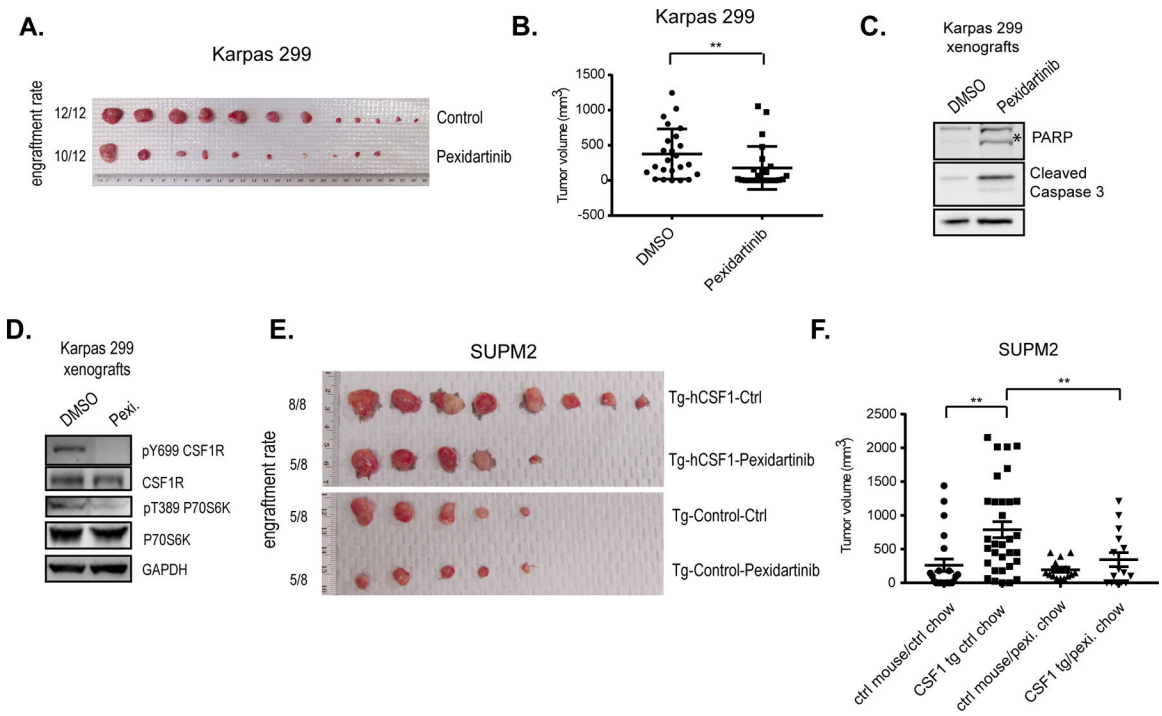

Figure 6.

CSF1 and CSF1R promote the growth of T-cell lymphoma xenografts. **A.** Representative photographs of tumor xenografts of Karpas 299 xenografts that secrete CSF1 and express CSF1R. Mice were feed with sham-chow (control) of pexidartinib-chow, the tumors were extracted after 10 days of treatment. Only tumors that displayed at least $1mm^3$ (volume) growth are included, the total number of tumors with more than $1mm^3$ tumor volume over the total number of engraftments is indicated (left). **B.** Graphic representation of the tumor volumes (mean +/− SD) after feeding the animals with sham-chow (control) or pexidartinib (n = 24). **C.** Protein extracts from Karpas 299 xenografts treated with control-chow (control) or pexidartinib were evaluated for PARP cleavage and Caspase 3 cleavage. Asterisk indicates cleaved PARP. Caspase 3 cleavage was evaluated with a specific antibody against cleaved Caspase 3. **D.** Phosphorylation of P70S6K (pT389) was evaluated from protein extracts of T-cell lymphoma xenografts (Karpas 299) by western blot analysis. GAPDH as loading control. **E.** Representative pictures of tumor xenografts of T-cell lymphoma lines that do not secrete CSF1 and express CSF1R (SUPM2). SUPM2 cells were injected in transgenic mice that secrete humanized CSF1 or control mice. Mice were fed either sham-chow (control) or pexidartinib-chow, the tumors were explanted 10 days later. Only tumors that displayed at least $1mm^3$ (volume) growth are displayed, the total number of tumors with $\geq 1mm^3$ tumor volume over the total number of injections is indicated (left). **F.** Graphic representation of the tumor xenograft volumes (mean +/− SD), comparing the effects of CSF1 and treatment with pexidartinib, are shown. **$p < 0.05$.

Table 1.

List of proteins within Pi3K-Akt signaling pathway with modifications upon CSF1R inhibition.

Pi3k-Akt pathway				
Gene symbol	**Protein name**	**p-residue**	**PLX/DMSO**	**p-value**
CSF1R	Macrophage colony-stimulating factor 1 receptor	Y699	0.67866667	0.0235544
IKBKG	NF-kappa-B essential modulator	S455	0.57060603	0.0089983
IRS1	Insulin receptor substrate 1	Y465,Y989	2.49579897	0.0443774
MAP2K2	Dual specificity mitogen-activated protein kinase kinase 2	S295	1.53823261	0.0435752
MCL1	Induced myeloid leukemia cell differentiation protein Mcl-1	T92	3.46612251	0.0125372
PKN2	Serine/threonine-protein kinase N2	T801	1.58048452	0.022626
PPP2R5C	Serine/threonine-protein phosphatase 2A	S458	0.57141452	0.0410022
RBL2	Retinoblastoma-like protein 2	S121,T988	0.43394198	0.0064254
SOS2	Son of sevenless homolog 2	T1232	0.31629528	0.0178266